Early movement restriction deteriorates motor function and soleus muscle physiology

Marie-Hélène Canu, Valérie Montel, Julie Dereumetz, Tanguy Marqueste, Patrick Decherchi, Jacques-Olivier Coq, Erwan Dupont, Bruno Bastide

Submitted to: EXPERIMENTAL NEUROLOGY (RESEARCH ARTICLE)

Early movement restriction deteriorates motor function and soleus muscle physiology

CANU Marie-Hélène[a*], MONTEL Valérie[a], DEREUMETZ Julie[a], MARQUESTE Tanguy[b], DECHERCHI Patrick[b], COQ Jacques-Olivier[b], DUPONT Erwan[a], BASTIDE Bruno[a]

Affiliations

[a] Univ. Lille, Univ Artois, Univ Littoral Côte d'Opale, ULR 7369, URePSSS – Unité de Recherche Pluridisciplinaire Sport Santé Société, F–59000 Lille, France.

[b] Institut des Sciences du Mouvement (ISM), Team 'Plasticité des Systèmes Nerveux et Musculaires', UMR 7287 CNRS, Aix-Marseille Université, Campus Scientifique de Luminy, F-13288 Marseille Cedex 09, France.

ORCID

MH Canu 0000-0003-4035-9619 / E Dupont 0000-0003-0777-9734 / JO Coq 0000-0002-3116-349X
B Bastide 0000-0002-7544-463X

Corresponding author

Marie-Hélène Canu, Eurasport, 413 rue Eugène Avinée, 59120 Loos, France,
marie-helene.canu@univ-lille.fr

Abstract

Children with low physical activity and interactions with environment experience atypical sensorimotor development and maturation leading to anatomical and functional disorganization of the sensorimotor circuitry and also to enduring altered motor function. Previous data have shown that postnatal movement restriction in rats results in locomotor disturbances, functional disorganization and hyperexcitability of the hind limb representations in the somatosensory and motor cortices, without apparent brain damage. Due to the reciprocal interplay between the nervous system and muscle, it is difficult to determine whether muscle alteration is the cause or the result of the altered sensorimotor behavior. (Canu et al., 2019). In the present paper, our objectives were to evaluate the impact of early movement restriction leading to sensorimotor restriction (SMR) during development on the postural soleus muscle and on sensorimotor performance in rats, and to determine whether changes were reversed when typical activity was resumed. Rats were submitted to SMR by hind limb immobilization for 16h / day from birth to postnatal day 28 (PND28). *In situ* isometric contractile properties of soleus muscle, fiber cross sectional area (CSA) and myosin heavy chain content (MHC) were studied at PND28 and PND60. In addition, the motor function was evaluated weekly from PND28 to PND60. At PND28, SMR rats presented a severe atrophy of soleus muscle, a decrease in CSA and a force loss. The muscle maturation appeared delayed, with persistence of neonatal forms of MHC. Changes in kinetic properties were moderate or absent. The Hoffmann reflex provided evidence for spinal hyperreflexia and signs of spasticity. Most changes were reversed at PND60, except muscle atrophy. Functional motor tests that require a good limb coordination, i.e. rotarod and locomotion, showed an enduring alteration related to SMR, even after one month of 'typical' activity. On the other hand, paw withdrawal test and grip test were poorly affected by SMR whereas spontaneous locomotor activity increased over time. Our results support the idea that proprioceptive feedback is at least as important as the amount of motor activity to promote typical development of motor function. A better knowledge of the interplay between hypoactivity, muscle properties and central motor commands may offer therapeutic perspectives for children suffering from neurodevelopmental disorders.

Keywords

Disuse / sensorimotor restriction / development / muscle contractile properties / muscle morphology / motor behavior /

Abbreviations

BW: body weight
C: control
CNS: Central nervous system
CP: cerebral palsy
CSA: cross sectional area
DCD: developmental coordination disorder
FI: fatigue index
HRT: half-relaxation time
MHC: myosin heavy chain
MWW: muscle wet weight
P_0: peak tetanic tension obtained at 100 Hz
PND: postnatal day
P_t: twitch peak tension
RH: right hind paw
SMR: sensorimotor restriction
TTP: time-to-peak

INTRODUCTION

Besides sedentary behavior, which is more and more frequent in our societies, acute and prolonged inactivity has deleterious effects on motor function and represents a public health issue (Hermans and Van den Berghe, 2015; Koukourikos et al., 2014). This issue is particularly acute when hypoactivity is experienced during development, for example in children who are bedridden due to chronic illness or accident. In the same line, children with either disabling motor disturbances, such as cerebral palsy (CP) or motor difficulties, like developmental coordination disorder (DCD), are less prone to be physically active and to interact with people and the environment. CP is the most common physical disability in children and involves a group of disorders of movement and posture, including spasticity in 85 to 91% of cases, and is often associated with behavioral and cognitive disorders. CP is mainly caused by a lesion, interference or abnormality originated in the immature brain (Coq et al., 2019; Rosenbaum et al., 2007). DCD refers to a developmental disorder of motor function with reduced abilities to produce consistent movements, poor motor coordination and somesthetic acuity, and broad impairments in sensorimotor representations and perception, reflected by disrupted central networks in the absence of apparent brain damage. DCD is usually associated with hyperactivity, and other behavioral and cognitive comorbidities (Biotteau et al., 2020; Coq et al., 2019). Children suffering from either CP or DCD have in common reduced physical activity and interactions with their environment, and thus xperience atypical sensorimotor development and maturation (Vaivre-Douret et al., 2016). Early hypoactivity usually leads to muscle atrophy, altered force production and endurance, spasticity, bone impairment, less complex and fluent movements (Jeffries et al., 2016; Li et al., 2011), and consequently to atypical motor development (Biotteau et al., 2020; Vaivre-Douret, 2014).

It is well established that physical activity and interactions with the environment are required at the earliest developmental stages for typical and harmonious maturation of the organization and functions of the central nervous system (CNS) (Luhmann et al., 2016). During typical development, the repertoire of general movements in limbs increases over time in variation, fluency, amplitude and complexity into a continuous stream of small and elegant movements. Atypical motor development and impaired functional connectivity or functional brain disorganization are reflected by the appearance of atypical spontaneous or general movements (Hadders-Algra, 2018; Vaivre-Douret et al., 2016). Atypical general movements correspond to rigid, cramped synchronized and stereotyped movements which exhibit limited fluency, variation and complexity with increasing age. Arising from spontaneous, self-generated and evoked movements during maturation, early somatosensory feedback drives electrical activity patterning from the spinal cord to the cortex. This feedback guides the development and refinement of the anatomical and functional organization of the sensorimotor circuitry, including most adapted movement repertoires (Hadders-Algra, 2018; Khazipov and Buzsáki, 2010; Zuk, 2011). Thus, prolonged hypoactivity might also induce secondary complications that occur over time as a result of primary impairment. In fact, many children who experience atypical sensorimotor activity will retain long-term motor difficulties during adulthood (Cousins and Smyth, 2003). However, it is difficult to determine whether CNS abnormalities are the cause or the result of the motor disturbances due to the reciprocal interplay between CNS and musculoskeletal system (Canu et al., 2019). Thus, we hypothesized that limited and abnormal patterns of

somatosensory inputs during development may lead to anatomical and functional disorganization of the sensorimotor circuitry in adults through maladaptive brain plasticity. In return, such disorganization may alter somatosensory and bodily perceptions, motor outputs and muscle structure and physiology (Delcour et al., 2018a; Delcour et al., 2018b).

Based on atypical movements and disrupted sensorimotor development, we developed a rat model of functional brain disorganization induced by early movement deprivation leading to sensorimotor restriction (SMR) during development (Coq et al., 2008; Strata et al., 2004). Briefly, hind limb immobilization from birth to postnatal day 28 (PND28) resulted in adult rats to digitigrade locomotion (i.e., "toe walking" or *pes equinus* observed in children with CP) related to ankle-knee overextension, degraded musculoskeletal histopathologies (e.g., gastrocnemius atrophy, joint degeneration and tibial bone shortening), and hyperexcitability in the lumbar spinal cord. The postnatal SMR also led to functional disorganization of the hind limb representations in the primary somatosensory and motor cortices, altered cortical response properties and cortical hyperexcitability, but without apparent brain damage, all signs of maladaptive cortical plasticity related to early atypical sensorimotor experiences (Coq et al., 2019; Delcour et al., 2018a; Delcour et al., 2018b).

In the present paper, our first objective was to characterize the enduring impact of SMR from birth to PND28 on one postural muscle, the soleus, and on sensorimotor performance in rats. Secondly, we examined whether a return to normal levels of activity during a one-month recovery period could restore the sensorimotor performance and muscle characteristics. We demonstrated that SMR induced a delay in muscle maturation and severe muscle atrophy that persisted over time. The force development, *in vivo* or *ex vivo*, was poorly affected but performance in motor tests which require good limb coordination showed enduring perturbation.

MATERIAL AND METHODS

Animals

All procedures described below were carried out in accordance with the European Communities Council Directive 2010/63/UE, and were approved by the Regional Committee on the Ethics of Animal Experiments of the Nord Pas-de-Calais region (CEEA 75, reference number: APAFIS#4732-2016031 112395755v7) and in Marseille (CEEA 71, reference number: APAFIS#20829-2019051718013359v11). All efforts were made to minimize the number of animals and their suffering.

Female and male OFA-Sprague-Dawley rats were purchased from Charles River Laboratories (L'Arbresle, France) and were housed in standard plastic cages in controlled conditions of humidity, temperature and light (22°C, 51% humidity, 12:12-h light-dark cycle). They had *ad libitum* access to water and food. Rats underwent at least 1 week of acclimatization after reception into the animal facility.

After mating with a male rat, pregnant female rats were transferred into individual cages and were pseudo-randomly assigned to two groups: control (C) or sensorimotor restriction (SMR). At parturition (post-natal day 0, PND 0), litter size was adjusted to 10 pups per dam. Body weight of pups was assessed daily from PND0 to PND28, then weekly until PND60. To obviate any litter effects, animals were randomly chosen from different litters. We used a total of 37 C and 33 SMR rats, obtained from respectively 10 and 9 litters.

Hind limb immobilization

The feet of the SMR pups were first gently bound together with medical tape. Their hind limbs were then immobilized in extended position and taped to a cast, made of hand-moldable epoxy putty sticks as previously described (Delcour et al., 2018a) (Fig. 1). These casts were well tolerated by the pups and mothers, and allowed the pups to move at the hip, urinate, defecate and to receive maternal care. After casting, pups were returned to their mother and littermates during the dark phase of day, corresponding to daily peaks of motor activity. During the day's light phase, the casts were removed so that pups could move freely for 8 h/day. After daily uncasting, the hind limb joints were passively moved through their full range of motion. The size of the casts was adapted to the growth of the rats from PND1 to PND28. To minimize the possible impact of stress induced by the casting, hind limb immobilization and maternal separation, C rats received comparable handling.

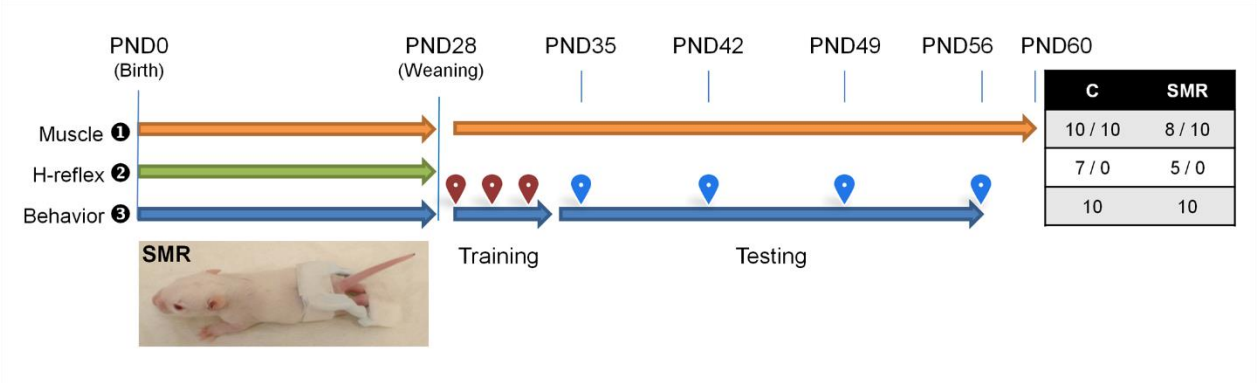

Figure 1. Experimental timeline showing the design and order of tests and sample sizes. Three sets of animals were used. For the set ❶, animals were submitted to contractile study at PND28 or PND60, and muscles were then removed for morphological and western blot analyses. Rats from the set ❷ were sacrificed at PND28 after Hoffmann reflex recording. All animals of the set ❸ were submitted to behavioral testings. The behavioral protocol included three training sessions (brown dots) followed by testing sessions once a week for rotarod, paw withdrawal, catwalk, grip test and activity wheels (blue dots). The photo on the left panel shows a young rat submitted to postnatal hind limb immobilization leading to SMR. The right panel indicates the number of animals at PND28 / PND60 per set. The same rats were tested in the behavioral analysis from PND35 to PND56.

Muscle analysis

Muscle evaluation (contractile properties, western blot and immunohistochemistry) was performed on a set of 38 rats, at PND 28 (10 C and 8 SMR) and PND60 (10 C and 10 SMR) (Fig. 1).

***In situ* isometric contractile properties of the soleus muscle and muscle removal.** At PND28 or PND60, the rats were deeply anesthetized with intraperitoneal injections of ketamine (50 mg·kg^{-1}) and dexmedetomidine (Domitor, 0.25 mg·kg^{-1}), prolonged if necessary by supplementary doses. The dissection protocol was previously described (Picquet and Falempin, 2003). Briefly, all the muscles of the right hind limb were denervated, except the soleus muscle. Then, the limb was fixed in isometric conditions and was immersed in a bath of paraffin oil thermostatically controlled (37°C). The limb was stabilized by using a combination of bars and pins, and the soleus muscle was maintained in a horizontal position. Afterward, the soleus muscle was isolated from surrounding tissues, and its distal tendon was connected to a force transducer (Grass FT 10; Grass Instruments, West Warwick, RI, USA). The muscle length was adjusted to produce a maximal twitch peak tension (P_t). Contractions were induced by stimulating the sciatic nerve (0.2-ms pulses) through bipolar platinum electrodes at least 1.5 × minimum voltage required to obtain the maximal twitch response. The following parameters were recorded: P_t, time-to-peak (TTP), half-relaxation time (HRT); peak tetanic tension obtained at 100 Hz (P_0). The ratio of subtetanic tension at 20 Hz relative to P_0 (P_{20}/P_0) was used as an indicator of muscle type; a low value (0.20 - 0.30) is characteristic of a fast muscle whereas a high value (0.70 - 0.80) indicates a slow muscle. The fatigue index (FI) was calculated as the percentage of the initial tension divided by the force at the end of the fatigue protocol in a series of 120 consecutive contractions (330 ms duration, 40 Hz, one train per second). At the end of the recording session, the muscle was removed, weighted and frozen in isopentane precooled to its freezing point by liquid nitrogen and stored at -80°C until histochemical and electrophoretic analyses. The rat then received a lethal dose of sodium pentobarbital (100 mg·kg^{-1}).

Western blot. Muscle contractile phenotype was determined through analysis of MHC composition. Myofibrillar proteins were extracted from muscle powder in a buffer containing 6.3 mM EDTA (pH 7) and anti-proteases (Complete EDTA-free, Roche Diagnostic), and centrifuged at 13,000 rpm for 10 min at 4°C, as previously described (Toursel et al., 2000). The pellet was washed twice in a 50 mM KCl buffer and dissolved in SDS sample buffer without 5% b-mercaptoethanol [62.5 mM Tris/HCl, 10% glycerol (vol/vol), 2% SDS (wt/vol), 0.02 bromophenol blue (wt/vol), pH 6.8]. The protein concentration was determined by using the Bradford protein estimation method before the addition of 5% b-mercaptoethanol (vol/vol) to the sample buffer and was stored at -80°C.

The MHC composition was determined by SDS-PAGE on a 7.5% separating polyacrylamide gel. Electrophoresis was run for 22 h at 12°C (180 V constant 13 mA per gel). Then the gels were sensitized with glutaraldehyde and silver stained. GS-800 Imaging densitometer and QuantityOne Software (Bio-Rad, Hercules, CA) were used to determine the relative proportions of the different MHC isoforms in each muscle. Slow (MHC I) and fast (MHC IIA, IID/X, and IIB) isoforms were identified according to their migration and previous reports of the laboratory (Dupont et al., 2011). The neonatal MHC isoform was identified using immunoblot analysis with a monoclonal antibody (sc-53097, Santa-Cruz Biotechnology Inc). After separation, proteins were transferred to 0.45-µm nitrocellulose membranes (Hybond, GE

Healthcare) using transfer buffer (20 mM Tris base; 150 mM glycine; 20% methanol), added with 0.025% SDS for the transfer of high-molecular weight proteins. Protein load and quality of transfer were verified by Ponceau staining. The blots were then washed in TBST (15 mM Tris/HCl, pH 7.6; 140 mM NaCl; 0.05% Tween-20) and blocked in 5% non-fat dry milk in TBST. Membranes were then blotted with primary antibody against neonatal MHC overnight at room temperature (RT) at 4 °C. Membranes were washed 3×10 min in TBST, and then incubated with HRP labelled secondary antibodies in blocking solution for 2h at RT followed by 5×10 min washes in TBST. Chemiluminescence detection was carried out using ECL Clarity (Biorad), and images capture were done with ChemiDoc MP (Biorad). For actin expression, proteins were separated on Criterion 12% Stain-Free precast polyacrylamide gels (Biorad); an internal standard was loaded on each gel. Stain-Free technology contains a proprietary trihalo compounds which react with proteins, rendering them detectable with UV exposure. Stain-Free imaging was performed using ChemiDoc MP Imager and Image Lab 4.0.1 software (Biorad) with a 5-min stain activation time, and total protein images were therefore obtained for protein expression normalization. All images were analyzed using Image Lab 4.0.1.

Histochemistry. The fiber cross-sectional area (CSA) was examined in 5 rats per group. Immunofluorescent staining was carried out on frozen sections (10 µm) of muscle. In summary, sections were incubated for 60 min at 37 °C with BSA (Bovine Serum Albumine, Sigma Aldrich) diluted to 3% in PBS (Phosphate Buffered Saline, Sigma Aldrich). They were then incubated for 60 min with a primary antibody cocktail containing laminin IgG (1:100, L9393; Sigma Aldrich), MHC I (1:100, BA-D5, Developmental Studies Hybridoma Bank -DSHB), MHC IIA (1:100, SC-71, DSHB) and MHC IIB (1:100, BF-F3, DSHB) antibodies at 4 °C, followed by three rinses. Fluorescence-conjugated secondary antibodies against Alexa Fluor 405 (1:250, A31556, InVitrogen), Alexa Fluor 647 (1:250, 1091-05, Southern Biotech), Alexa Fluor 488 (1:250, RMG1-1, Bio-legend) and Alexa Fluor 555 (1:250, 1021-30, Southern Biotech) were applied for 30 min at RT in obscurity. Finally, the sections were mounted in ProLong Gold Antifade Mountant (P36934, Invitrogen) and coverslipped. Images were acquired using a Leica-DMI8 inversed microscope, fitted with an automated motorized platform for mosaic imaging with the LAS X software (Leica). Muscle fiber CSA was determined using the MuscleJ plugin (Mayeuf-Louchart et al., 2018). On average, 1418 fibers were analyzed for each muscle. CSA smaller than 125 µm² and larger than 3500 µm² for PND28 rats (350 and 7000 µm² for PND60 animals respectively) were excluded from this analysis. These values correspond to the smallest and largest fibers found by manual observation.

Rate dependent depression

The Hoffman reflex (H-reflex) was measured in a set of PND28 rats[1] from both groups (7 C and 5 SMR), as already described (Delcour et al., 2018a). Briefly, rats were maintained under deep anesthesia, induced first with isoflurane and then with ketamine (100 $mg \cdot kg^{-1}$ i.p. induction) and maintained with supplemental doses of ketamine (20 $mg \cdot kg^{-1}$ i.p.). A transcutaneous pair of stimulating needle wires was

[1] This experiment has been performed at PND28 only due to the Covid-19 pandemia.

inserted around the peroneal branch and a pair of stainless steel recording electrodes was inserted into the gastrocnemius muscle. A reference electrode was placed into the skin. First, we stimulated the peroneal branch for 0.2 ms at 0.2 Hz with increasing current intensities until the maximum M wave stabilized, and determined the intensity required for a maximal H response. The peroneal branch was stimulated with trains of 20 stimulations at 0.2, 0.5, 1, 2, and 5 Hz with 2-min intervals between each train. For each frequency, the responses were averaged, while discarding responses to the first three stimulations required for the depression to occur. The M and H waves were rectified and the areas under the curves were measured. The H responses were expressed as percentages relative to the mean response at 0.2 Hz within the same series of measurements.

Behavioral assessment

Behavioral assessment has been performed in a set of 20 rats (10 C and 10 SMR). The same rats were tested once a week from PND35 to PND56 (Fig. 1). The training session was reduced to avoid lack of interest. The total time to perform the tests (rotarod, grip test, paw withdrawal and footprint) was estimated about 1 h par session. Tests were adapted from Brooks and Gunnett, 2009,) Maurissen et al. 2003 and Martinov et al., 2013.

Rotarod task. The motor coordination of rodents was evaluated by using the rotarod test (Bioseb). Training began when rats were 28 days old. In the training trials, the rat was placed on the rod (7 cm diameter), which was rotating at a constant speed of 15 rpm. Habituation was repeated every day for 3 days before the testing sessions. Testing was conducted once per week from PND28 to PND56. The rod was accelerated from 5 to 40 rpm over 180 s and then was left at constant speed. Rats were left on the rotating rod until they fall down and the latency to fall was recorded.

Grip Test (Bioseb, France). Rats were habituated to the apparatus for 3 days. The animals were gently supported by the experimenter at armpit level and the hind paw brought into contact with the bar. When they grasped the metal bar, their body was gently moved backwards until they dropped the bar. The dynamometer measured the maximal isometric force before the animal released the bar. Each testing session consisted of 5 successive trials, which duration did not exceed 5 s. The force applied to the apparatus was checked on a computer screen. Trials where the force did not increase regularly, following a ramp force (force/time), were rejected. The results are expressed as the mean of the 5 values in grams (g), and normalized to the body weight (g/g). Because this test requires extensive handling of rats, all tests were performed by the same experimenter.

Paw withdrawal threshold (electronic Von Frey hair unit, Ugo Basile, Italy). The animals were placed in 20 × 20-cm Plexiglas boxes equipped with a mesh floor. After a 10-min period of habituation, the withdrawal threshold was evaluated by applying a force ranging from 0 to 1000 g. Stimulus was delivered to the midplantar area of both left and right hind paws. The force was displayed on the computer screen. Only trials with regular linearly increasing force and clear paw withdrawal were taken into account. The measure was repeated until recording 6 successful trials, with an interval of at least 10 s between trials. The final value was obtained by averaging the 5 measurements than deviate the least from the median (Martinov et al., 2013).

Footprint analysis. The walking characteristics were analyzed with the Catwalk system (CatWalk XT, Noldus Information Technology, Netherlands). Rats were trained prior to recording for 3 days. Rats were allowed to freely run across an enclosed walkway illuminated by fluorescent light (width: 5 cm; length: 100 cm). Footprints were digitized with a high-speed color camera (10 frames·s^{-1}) connected to a computer. Five runs were collected per rat and per day. The right hind paw (RH) was taken as a reference. The following parameters were quantified: step cycle duration (time between two consecutive initial contacts of RH), duration of the stance and swing phases and duty cycle; stride length; body speed; max contact (time that paw makes maximum contact with the glass plate expressed as a percent of the stand phase for RH; footfall patterns (order in which the paws were placed on the walkway). Predefined paw sequences are cruciate (e.g. right forepaw - left forepaw - right hindpaw - left hindpaw and so on), alternate (e.g. right forepaw - right hindpaw - left forepaw - left hindpaw) and rotate (e.g. right forepaw – left forepaw – left hindpaw – right hindpaw). For each rat and each day, a value was determined, that corresponded to the mean of at least 10 steps.

Running wheel. Spontaneous wheel-running activity was recorded for a 2-hour session (during the light phase; session started between 10 AM and 12 AM) using activity wheels designed for rats (model BIO-ACTIVW-R, Bioseb). Rats were placed into polycarbonate cages (20 × 35 × 13 cm) with free access to stainless steel activity wheels (diameter 34 cm; lane width 7 cm). The wheel could be turned in both directions. Wheels were connected to a computer that automatically recorded the spontaneous activity by means of ACTIVW-SOFT software (Bioseb). The average and maximum speed and total active time were measured for each rat. The test was conducted at PND35, PND42, PND49 and PND56.

Data analysis

All data are expressed as mean ± SEM. Statistical analysis was performed by using Prism software (GraphPad, USA). Data normality was determined with the Shapiro-Wilk test. Afterward, we applied either parametric or non-parametric tests. Pairs were tested with t-tests or Mann-Whitney. For more than two groups, one-way or two-way ANOVA with Tukey or Sidak *post-hoc* test was used. The type of statistical test is indicated in each figure or table legend. Values of $P<0.05$ were considered statistically significant.

RESULTS

By PND28, no difference in morphologic and force-related parameters was noticed between males and females. Thus, both sexes were pooled. At contrast, at PND60, these parameters are known to be highly dependent on sex (Drzymala-Celichowska et al., 2012; Drzymała-Celichowska and Krutki, 2015). As a consequence, whenever possible, groups were evaluated separately by using a two-way ANOVA with *sex* and *group* as between factors.

Morphological parameters

At birth, the body weight (BW) was comparable in the C and SMR groups (respectively 6.59 ± 0.06 and 6.58 ± 0.20 g). At PND28, SMR rats exhibited growth retardation. Their BW was lower (-23%, $p<0.001$) than that of C rats (Table 1). The difference between groups became significant from PND22 (Fig. 2). The

BW recovered by PND60, since no difference was measured between the two groups. However, a great difference was observed between male and female rats in C ($P<0.01$) as in SMR group ($P<0.01$) at PND60.

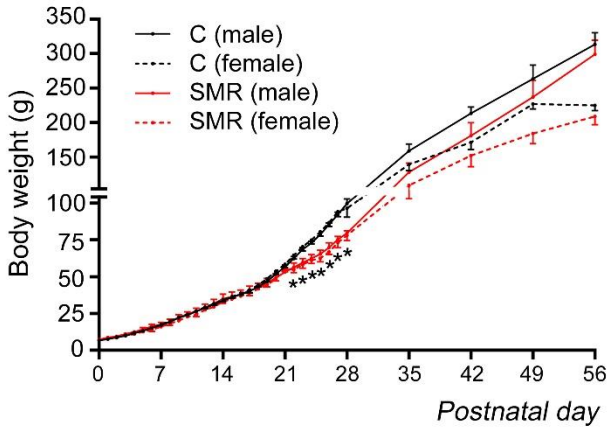

Figure 2: Increases of body weight over time according to group and sex. Values are mean ± SEM. Statistical significance was determined by multiple t-tests with correction for multiple comparisons using the Holm-Sidak method. *: $p<0.001$ with respect to C rats.

A severe atrophy of the soleus muscle was noticed in the SMR group, whatever the age and sex (Table 1). This atrophy was highlighted by a decrease in muscle wet weight (MWW; PND28: -39%, $p<0.001$; PND60: -38% males, -44% female, $P<0.001$), which cannot be explained by the growth retardation, since it persisted when MWW was normalized to BW (PND28: -24%, $p<0.001$; PND60: -38% males, -41% female, $P<0.001$).

The fiber CSA was studied in a total of 20 muscles at PND28 (5 C and 5 SMR) and PND60 (5 C and 5 SMR). No difference was detected between males and females ($p=0.68$). The mean CSA was decreased in SMR rats with respect to C ones (PND28: -29%, $p<0.01$) but recovered partially at PND60 (-14%, $p=0.09$). The χ^2 analyses showed that the CSA was lower in SMR animals compared to C ones at PND28 (Fig. 3). At PND60, the profile was quite similar in both groups except that higher values (>3000 μm^2) were more represented in the SMR group.

TABLE 1: morphological parameters

		BW (g)		MWW (mg)		MWW/BW (mg/g)	
		Controls	**SMR**	**Controls**	**SMR**	**Controls**	**SMR**
PND28		100 ± 3	77 ± 2 ***	38 ± 2	23 ± 1 ***	0.38 ± 0.02	0.29 ± 0.01 ***
PND60	**Male**	313 ± 16	310 ± 21	127 ± 6	78 ± 5 ***	0.41 ± 0.01	0.25 ± 0.01 ***
	Female	224 ± 7	214 ± 10	106 ± 8	59 ± 4 ***	0.47 ± 0.03	0.28 ± 0.02 ***

PND28: 10 C and 8 SMR. PND60: 10 C (5 males and 5 females) and 10 SMR (5 males and 5 females).
BW: body weight, MWW: muscle wet weight. Values were compared with Mann-Whitney test at PND28 and two-way ANOVA with sex and group as between factors at PND60 (Tukey's multiple comparison test). *** different from C group at the same age (PND28) or at the same age and sex (PND60) ($P< 0.001$). Values are mean ± SEM.

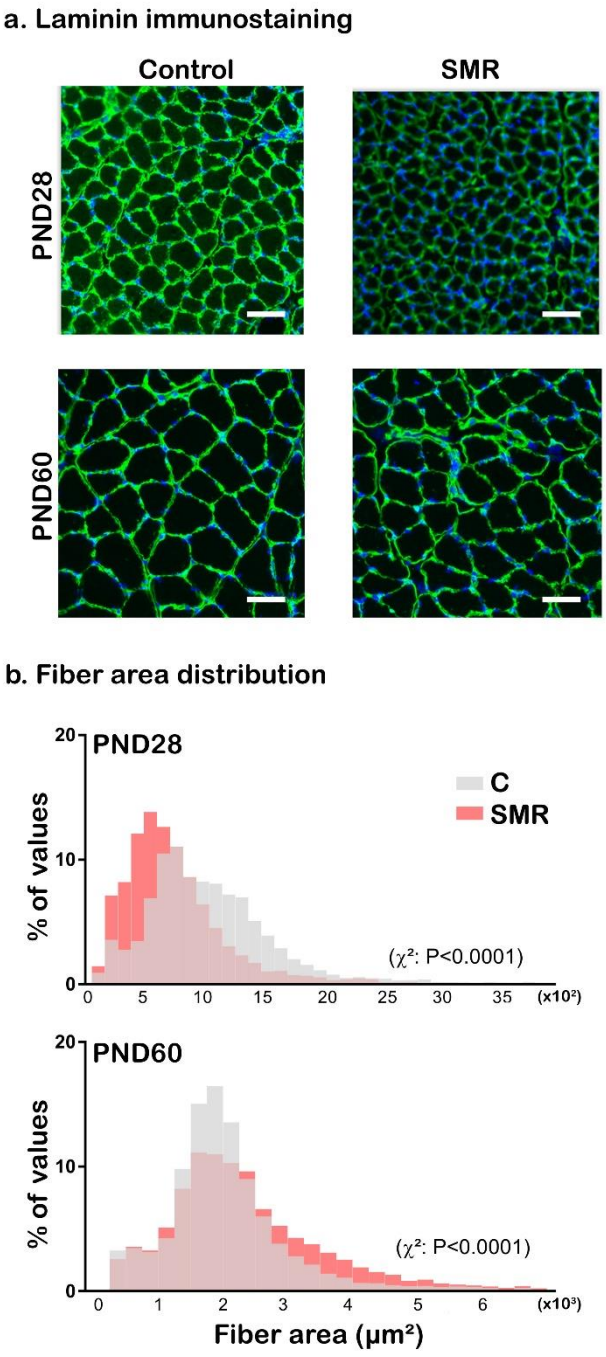

Figure 3: Fiber cross-sectional area (CSA) for soleus muscle of control (grey) and SMR (red) rats, at PND28 and PND60. a. Microphotographs showing cross-sections of the soleus muscle after immunostaining of laminin (green) and DAPI (blue). Scale bar: 50 µm. b. Overlay histograms presenting frequency distribution of CSA for C and SMR rats. Bin width are 100 µm² and 200 µm² at PND28 and PND60 respectively. The CSA of SMR fibers was lower at PND28 (χ^2=1751; P<0.0001). At PND60, large fibers (>3000 µm²) were more represented (χ^2=410.2; P<0.0001).

Contractile and kinetic parameters

Twitch tension (P_t) was decreased in SMR at PND28 (-39%, p<0.01) compared to controls (Table 2). However, when expressed relative to muscle weight, values were comparable. At PND60, a group effect was still present for P_t [F(1,16)=9.86; P<0.01] (males: -23%, females: -38%), whereas Pt/MWW was unchanged [F(1,16) = 1.61; p=0.22, n.s.].

Maximal tetanic tension (P_0) was dramatically reduced in SMR rats at PND28 (-49%, p<0.001). A *group* effect was also observed at PND60 [F(1,16)=11.72; P<0.01] (males: -21%, females: -44%). This decrease was due to the muscle atrophy, since relative to muscle weight, the value was unchanged [F(1,16)=0.96; p=0.34, n.s.]. As a result, the twitch-to-tetanic ratio (P_t/P_0) was increased at PND28 (+20%, p<0.05) and recovered at PND60 [F(1,16)=0.24; p=0.63, n.s.].

TABLE 2: contractile parameters

		P_t (mN)		P_0 (mN)		P_t/MWW (mN/mg)		P_0/MWW (mN/mg)		P_t/P_0	
		C	SMR	C	SMR	C	SMR	C	SMR	C	SMR
PND28		8.1 ± 0.6	4.9 ± 0.6 **	63.6 ±4.21	32.2 ± 4.77 ***	0.22 ± 0.01	0.22 ± 0.02	1.71 ± 0.11	1.46 ± 0.19	12.7 ± 0.6	15.3 ± 0.6 *
PND60	**Male**	17.5 ± 2.0	13.5 ± 0.3	116.8 ± 16.1	92.7 ± 2.9	0.14 ± 0.01	0.17 ± 0.01	0.91 ± 0.11	1.21± 0.09	15.2 ± 0.4	14.6 ± 0.6
	Female	16.1 ± 0.9	10.0 ± 2.3	116.9 ± 5.5	65.9 ± 13.6 *	0.15 ± 0.01	0.18 ± 0.05	1.12 ± 0.09	1.15 ± 0.28	13.7 ± 0.6	15.2 ± 1.5

PND28: 10 C and 8 SMR. PND60: 10 C (5 males and 5 females) and 10 SMR (5 males and 5 females).
P_t: twitch tension, P_0: tetanic tension at 100 Hz, MWW: muscle wet weight. *, ** and *** different from controls at the same age and the same sex (for PND60 rats) (P<0.05, 0.01 and 0.001, respectively). PND28: unpaired t-test or Mann-Whitney; PND60: two-way ANOVA with Tukey's *post-hoc* test.

Kinetic parameters varied from PND28 to PND60, but no change was noticed between C and SMR rats (Table 3). At PND28, the P_{20}/P_0 ratio was low in C rats and reached the value of a fast muscle. At PND60, this parameter evolved towards a higher value, characteristic of a slow muscle. Values were similar for the SMR group. In the same way, TTP and HRT increased at PND60 with respect to PND28, but data were comparable in the C and SMR groups.

To sum up, changes in contractile and kinetic properties were moderate or absent after SMR, and can be mainly explained by muscle atrophy.

TABLE 3: kinetic parameters

		TTP (ms)		HRT (ms)		P_{20}/P_0		FI (%)	
		C	**SMR**	**C**	**SMR**	**C**	**SMR**	**C**	**SMR**
PND28		49 ± 2	51 ± 3	49 ± 3	52 ± 7	46 ± 3	49 ± 2	89 ± 3	97 ± 4
PND60	Male	75 ± 4	64 ± 2	63 ± 3	56 ± 3	68 ± 2	63 ± 1	82 ± 2	88 ± 4
	Female	69 ± 4	68 ± 6	61 ± 6	65 ± 7	61 ± 1	63 ± 5	81 ± 3	86 ± 4

PND28: 10 C and 8 SMR. PND60: 10 C (5 males and 5 females) and 10 SMR (5 males and 5 females).
TTP: time-to-peak, HRT: half relaxation time, P_0: tetanic tension at 100 Hz, P_{20}: tetanic tension at 20 Hz, FI: fatigue index. PND28: unpaired t-test or Mann-Whitney; PND60: two-way ANOVA with Tukey's *post-hoc* test.

Muscle myosin heavy-chain composition

The MHC expression of the whole soleus muscle was determined by Western blots and results are presented in Fig. 4. As expected, the MHC pattern of expression in C rats showed a predominance of type I (62%) and IIA (36%) MHC, with only traces of the fast IIB isoform for two muscles (0.1%). A small amount of neonatal form was still present (1.7%). In SMR rats at PND28, the proportion of MHC I was lower (49%; $p<0.05$) whereas the proportion of fast isoforms was increased, almost significantly (MHC IIA + IIB: 48%; $P=0.053$), compared to controls. The neonatal isoform was still present in one third of SMR subjects at a low level (3.2%). At PND60the muscle of controls evolved towards a slow-twitch type with an increase in slow isoform (82%, $p<0.001$), a decrease in MHC IIA isoform (18%, $p<0.001$) and a total disappearance of MHC IIB and neonatal forms (ns). In SMR rats, no difference was reported with respect to C rats at PND60.

The actin expression was also determined. The total expression was increased at PND60 with respect to PND28 [+38%, $F(1,24)=150.5$, $P<0.0001$], but no difference was noticed between C and SMR rats [$F(1,24)=2.1$; $P=0.16$, n.s.] (Fig. 4c).

The identification of muscle fiber type was also performed by immunohistochemistry. The quantitative data revealed that the soleus muscle of young C rats (PND28) contained 64% of type I fibers, 33% of fast type IIA fibers, and 3% of fibers co-expressing the two MHC isoforms, MHC I/MHC IIA. The amount of fibers expressing MHC I significantly increased at PND60 [*Time* effect: $F(1,13)=72.98$; $P<0.0001$] to reach 90%; whereas, IIA fibers were reduced at 8%. Values were very close in SMR rats (PND28: 68% of MHC I and 8% of MHC IIA; PND60: 91% and 8% respectively) [*Group* effect: $F(1,13)=0.19$; $P=0.67$, n.s.].

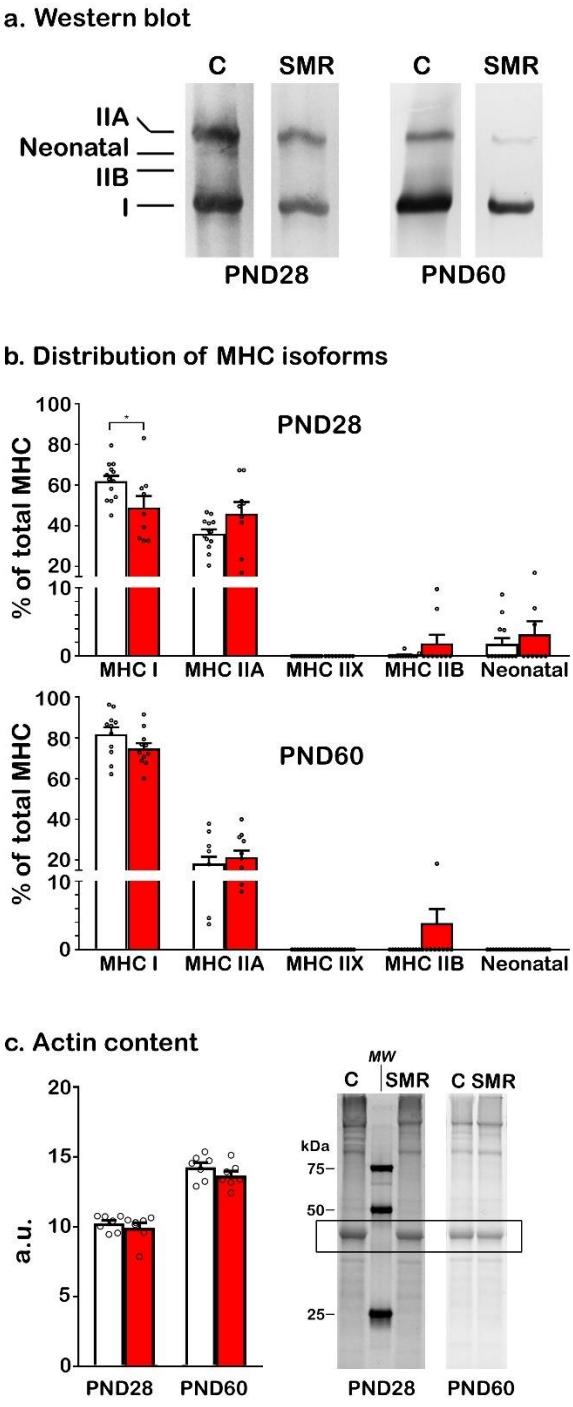

Figure 4. Electrophoretic determination of myosin heavy chain (MHC) isoforms in the soleus muscle of C and SMR rats at two ages (PND28 and PND60). (a) Representative western blot showing the MHC isoforms. (b) Distribution histogram of MHC isoforms. (c) representative Western blot and quantification of actin (normalized to the whole proteome, i.e., Stain Free signal). Data show a delay in

muscle maturation with persistence of neonatal isoform at PND28. Control: white bars. SMR: red bars. Dots are individual data points. *P < 0.05, Mann-Whitney. a.u. arbitrary unity, MW: molecular weight.

H-reflex and rate-dependent depression

The spinal H-reflex was used to determine whether SMR induced hyperreflexia in the lumbar spinal cord and spasticity within the hind limb. Increasing stimulation frequency was performed to determine the rate-dependent depression, i.e. the decrease in reflex magnitude relative to stimulation rate. M and H waves were expressed with respect to the value obtained at a baseline frequency of 0.2 Hz (Fig. 5).

The statistical analysis did not reveal significant difference between groups for M wave. At contrast, for H-reflex wave, a *group* effect [F(1,45)=47.15, P<0.001], a *frequency* effect [F(4,45)=7.02, P=0.001] and a *group* x *frequency* interaction [F(4,45)=3.18, P=0.05] were observed. In C rats, the H-reflex was depressed when the stimulation frequency was increased to reach 46% of baseline value at 10 Hz (P<0.001). In the SMR group, the depression was lower than in the C group: at 10 Hz, the H-wave amplitude was 91% of the value measured at 0.2 Hz and was not different from baseline, suggestive of the presence of hyperreflexia and spasticity in the gastrocnemius after SMR.

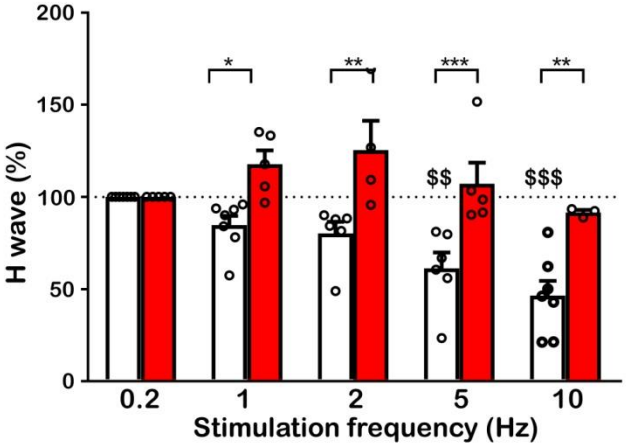

Figure 5. Amplitude of H waves in C and SMR rats at PND28. H waves are expressed with respect to the value obtained at baseline frequency of 0.2 Hz. The lower rate-dependent depression after SMR is indicative of hyperreflexia. Control: white bars. SMR: red bars. *, **, ***: P<0.05, 0.01 and 0.001 with respect to C group. §§ and §§§: p < 0.01 and 0.001 with respect to baseline value (i.e. 100%). Values were compared with two-way ANOVA, with group as between factor and frequency as within factor, Sidak's *post-hoc* test. Circles are individual data points.

Behavioral assessment

Qualitative observation revealed that SMR rats exhibited irregular steps, difficult limb coordination and knee and ankle hyperextension, corresponding to digitigrade locomotion, confirmed by locomotor kinematics analysis (Delcour et al., 2018a).

Muscle strength evaluation with the grip test (Fig. 6) revealed that the force was increased from one week to the other [*time* effect: F(3,54)=5.60; P<0.01] in controls?. In addition, values were always lower for SMR rats than for C rats [*group* effect: F(1,18)=21.77; P<0.001]. However, when normalized to body weight, the force decreased with *time* [F(3,54)=14.43; P<0,0001] and the *group* effect disappeared [F(1,18)=2.63; P=0.12]. It indicates that the force deficit in SMR rats was mainly due to their growth retardation rather than a deficit in muscle force production.

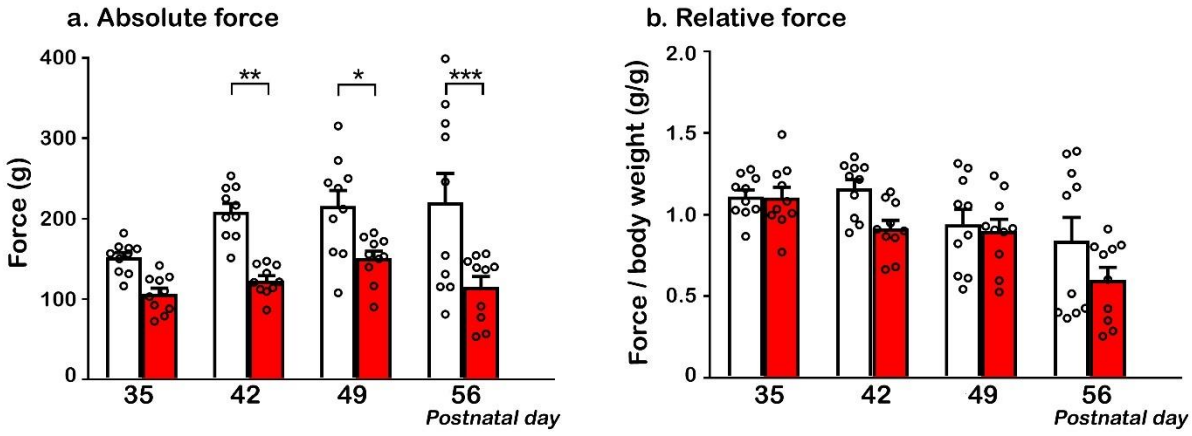

Figure 6. Performance on the grip test in control and SMR rats. Rats grasped a metal bar and their body was then gently moved backwards until they dropped the bar. For each animal and each recording day, the final value was obtained by averaging 5 measurements. (a) Histograms present the maximal isometric force. Rats of the SMR group developed less force than C ones [*time* effect: F(3,54)=5.60; P<0.01; *group* effect: F(1,18)=21.77; P<0.001]. (b) When the force was normalized to the body weight (g/g), the force decreased with time [F(3,54)=14.43; P<0.0001] and the *group* effect disappeared [F(1,18)=2.63; P=0.12]. Control: white bars. SMR: red bars. *,P<0.05; **, P<0.01; ***,P<0.001; two-way ANOVA with repeated measures and Sidak *post-hoc* test.

Motor coordination was evaluated by the rotarod test (Fig. 7). Rats were left on the rotating rod until they fall. SMR strongly affected motor coordination as shown by the decrease in the time spent on the rotating bar. Figure 7 presents the mean value for the different days. It clearly appears that the time-to-fall was reduced in SMR rats, compared to controls [*group* effect: F(1,18)=22.13;P<0.001]. In C rats, the duration varied between 15 s and 338 s; whereas, the maximum duration was only 79 s in SMR animals.

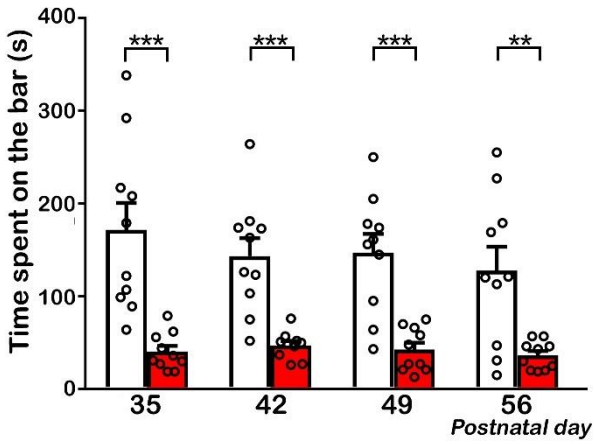

Figure 7. Motor coordination was affected in SMR rats. During performance on the accelerated rotarod test (5–40 rpm/3 min), SMR rats demonstrated an impaired ability to remain on the rod, compared with C rats [*time* effect: $F(3,54)=2.92$; $P<0.05$; *group* effect: $F(1,18)=22.13$; $P<0.001$]. Control: white bars. SMR: red bars. **, $P<0.01$; ***,< 0.001, two-way ANOVA with repeated measures and Sidak *post-hoc* test.

The behavioral response to mechanical stimulation of the hind paw was evaluated by using an electronic Von Frey. This test is frequently used to test allodynia and tactile sensitivity. However, when pushing on the hind limb, C as well as SMR rats sometimes seemed to be indifferent to the stimulation as they did not remove their paw, but the tip pushed on the paw so much that the paw lifted off the ground. In addition, paw withdrawal occurred within relatively large delay (370 ± 17 ms in C rats), which suggests that the tactile stimulus was non-noxious (Blivis et al., 2017). The threshold required to evoke paw withdrawal increased with time [+32% from PND35 to PND56 in C rats; +95% in SMR rats; *time* effect: $F(3,54)=6.58$; $P<0.001$]. SMR rats were more sensitive than C rats as the threshold was lower [-37% at PND35 and -8% at PND56; *group* effect: $F(1,18)=4.74$; $P<0.05$] (Fig. 8A). However, when paw withdrawal threshold was plotted against body weight (Fig. 8B), it seems that until a body weight of 180 g the threshold was proportional to the body weight and thus, the lower threshold could be explained by lower body weight due to growth delay.

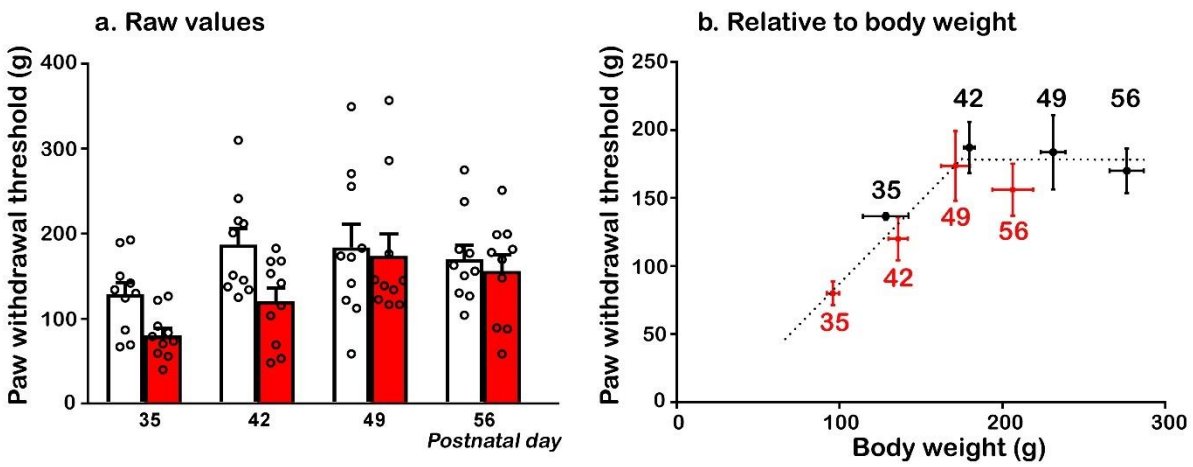

Figure 8. Paw withdrawal threshold is lower in young SMR rats. The tip of an electronic Von Frey was poked on the hind paw through the mesh and the force required to evoke a clear paw withdrawal were recorded. For each animal and each recording day, the final value was obtained by averaging the 5 measurements. (A) The threshold was lower in SMR rats for the early phase of recovery [*time* effect: $F(3,54)=6.58$; $P<0.001$; *group* effect: $F(1,18)=4.74$; $P<0.05$]. (B) In young rats until 180 g, paw withdrawal threshold was proportional to body weight. Thus, the lower threshold appeared mainly related to growth retardation. Control: white bars. SMR: red bars. Values are mean ± SEM. Circles are individual data points.

Analysis of the locomotor kinematics and patterns recorded using the Catwalk system (Fig. 9) reveals an increase (+20%) in swing duration in SMR rats, but no change in stance duration. Step cycle duration varied with time [$F(3,54)=12.7$; $P<0,001$]: in C rats, values increased from 0.29 s (PND35) to 0.40 s (PND56). No *group* effect was detected [$F(1,18)=0.19$; $P=0.67$]. A *time* effect was also observed for the duty cycle (corresponding to stand duration expressed as a percentage of step cycle) [$F(3,54)=11.47$; $P<0.001$] (Fig. 9B). In C rats, the duty cycle increased from 57% at PND35 to 66% at PND56. Moreover, this parameter was decreased in SMR rats (from -17% at PND35 to -26% at PND49). Maximum contact (Fig 9D), which corresponds to the point at which the braking phase turns into propulsion phase during stance, occurred later after the onset of stance phase: the value was ~27% in C rats; whereas, it increased to ~43% in the SMR group. Concerning the spatial parameter, stride length (Fig 9C) was near 13 cm in C rat and a small decrease was reported in the SMR group. The footfall pattern was categorized into 3 classes. By PND35, the 'alternate' and 'cruciate' patterns predominated in controls (59% and 39% respectively). The 'rotate' pattern was almost absent (<1%). This repartition was very stable over time. By contrast, the footfall pattern was different in SMR rats with a predominance of 'alternate' pattern (84%) at the expense of 'cruciate' one (11%). 'Rotate' pattern represented 3%. The difference in footfall patterns between C and SMR rats was significant.

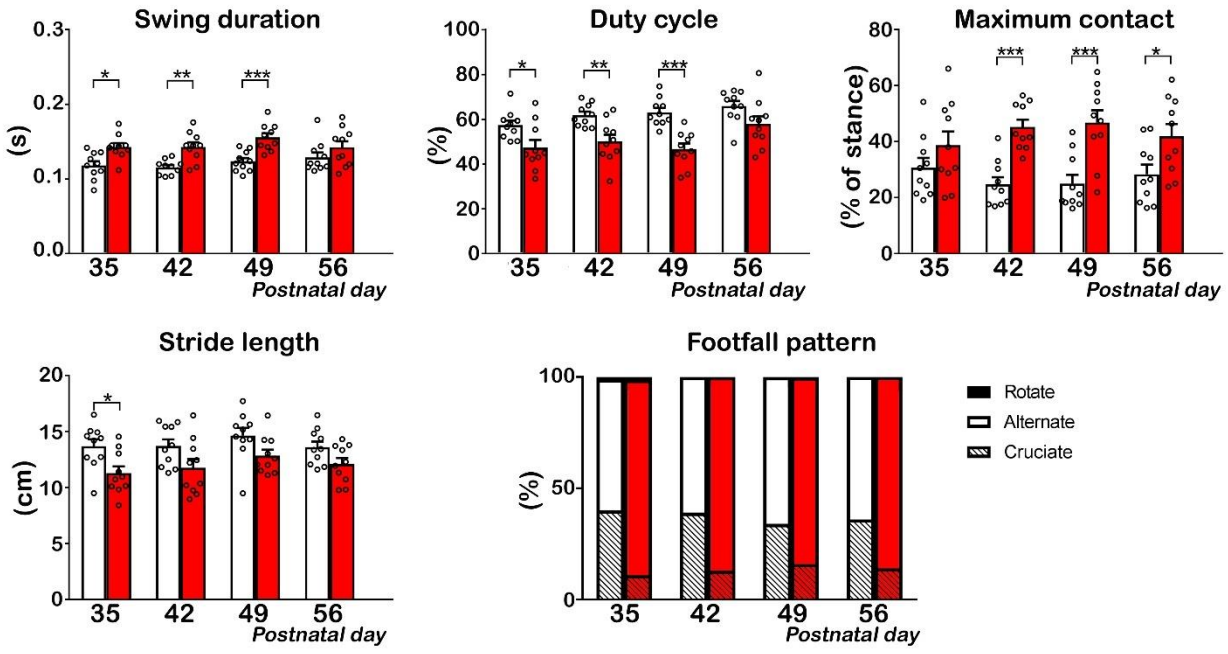

Figure 9. SMR induced enduring changes in locomotor patterns. Locomotor function was evaluated by using the Catwalk system. Swing duration was increased in SMR rats [F(1,18)=16.16; P<0.001] with no change in stance duration [-12%; F(1,18)=1.19, P=0.29]. As a consequence, the duty cycle [(stance duration / (stance + swing)) × 100] was lower [*Group* effect: F(1,18)=14.69; P<0.01]. Stride length was reduced in SMR rats [F(1,18)=8.61; P<0.01]. Maximum contact is the time that the hind paw makes contact with the floor, expressed as a % of stance phase duration [Max contact = (time of contact - time of stance onset) / stance duration) × 100]. Values were increased [F(1,18)=15.1; P<0.01], suggestiveof increased braking phase while the propulsion phase was shorter. The footfall pattern was changed durably towards a higher percentage of alternate pattern (χ^2=26.47 at PND35, P<0.001; χ^2=19.95 at PND42, P<0.001; χ^2=8.30 at PND49, P<0.05; χ^2=13.42 at PND56, P<0.01). Control: white bars. SMR: red bars. For each animal and each day, the value was an average for the step cycles. *, P<0.05; **, P<0.01; **,*P<0.001, two-way ANOVA with repeated measures and Sidak *post-hoc* test).

Finally, the spontaneous activity was assessed by giving the rat free access to activity wheels (Fig. 10). At PND35, the active time was almost similar for both groups (C: 1215 ± 512 s; SMR: 1109 ± 423 s) as well as the maximum speed (C: 58.2 ± 17.4 $m \cdot s^{-1}$; SMR 49.9 ± 9.7 $m \cdot s^{-1}$). For each rat, values were normalized with respect to that measured at P35. In C rats, active time and maximal speed were unchanged from PND35 to PND56 (+ 3% and +12% respectively). At contrast, values increased in SMR rats and reached significance at PND56 (active time: +45%; max speed: +49%), indicative of spontaneous locomotor hyperactivity.

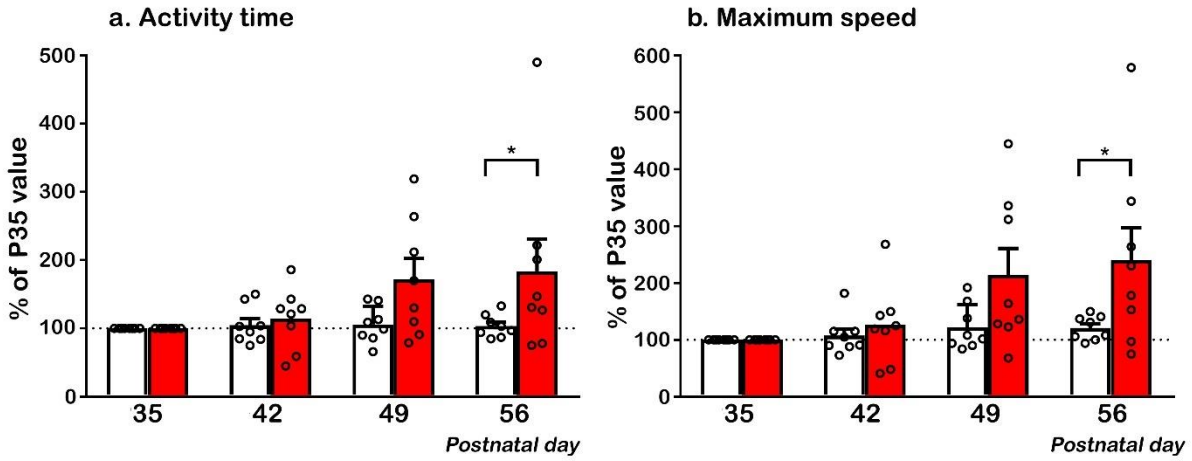

Figure 10. Spontaneous activity in running wheels increased in SMR rats. (A) The time spent in the running wheel was unchanged in C rats, but increased over time in SMR rats. [*time* effect: F(3,42)=2.55; P=0.07; *group* effect: F(1,14)=4.09, P=0.06]. (B) Maximum running speed was increased from PND35 to PND56 in SMR rats, but not in C rats [*time* effect: F(3,42)=2.50, P=0.07; *group* effect: F(1,14)=5.05, P<0.05]. Control: white bars. SMR: red bars. *, P < 0.05; two-way ANOVA with repeated measures and Sidak *post-hoc* test).

To sum up, motor tests that require a good coordination between intra- and inter-limbs during rotarod and locomotion showed enduring alterations related to SMR. No recovery was noticed after one month of 'typical' activity after SMR for most parameters. On the other hand, paw withdrawal test and grip test were poorly affected by SMR; whereas, spontaneous locomotor activity increased over time.

DISCUSSION

Our objectives were to evaluate the impact of early SMR on the postural soleus muscle and on sensorimotor performance in rats, and to determine whether changes were reversed when typical activity was resumed. Our main results are as follows: SMR induced an early and transient decrease in body weight and a severe muscle atrophy that persisted over time. The maturation of soleus muscle appeared delayed, with a greater persistence of neonatal forms of MHC at PND28. SMR induces severe changes in contractile properties that can be fully explained by muscle atrophy. In the same line, *in vivo* force development (i.e. grip test) was poorly affected by SMR, and changes in kinetic properties were moderate or absent. SMR rats also displayed hyperreflexia within the lumbar spinal cord and likely signs of spasticity at PND28. Finally, the overall activity in running wheels was similar at PND28 and increased thereafter, but sensorimotor tests that require a good intra- and inter-limbs coordination (rotarod, locomotion) showed an enduring alteration after SMR.

Studies examining the deleterious impact of transient immobilization or disuse have been mainly conducted in adult animals. However, despite the relevance of this topic, consequences of disuse during

growth on the neuromuscular system and motor performance have been only poorly studied. In young rodents, hind limb unloading or restricted range of motion induces altered muscle physiology and phenotype (Huckstorf et al., 2000; Kawano et al., 2010; Picquet et al., 1998; Serradj et al., 2013), bone structure (Miranda et al., 2016) and changes in the locomotor pattern (Walton et al., 1992; Westerga and Gramsbergen, 1993). In these studies, rodents were immobilized by casting or hind limb unloading, from a few days to 2 months, at various periods of development, but the severity and duration of impairment is related to the age at which the animals were immobilized and the duration of immobilization (Walton et al., 1992). In addition, muscle properties and motor function were rarely studied together, and whether they can recover is unclear. Interestingly, one study performed in mice suggests that motor performance in adults (9 months) is dependent on motor activity during a defined period of motor development (PND10 to PND30) (Serradj et al., 2013).

1. SMR induces an enduring muscle atrophy and force loss

The decrease in BW occurred only at P22, i.e. at the beginning of weaning. This decrease is likely due to difficulties for accessing food rather to a difficulty accessing the mother's nipples and/or to a stress induced by manipulation. Indeed, maternal separation during the early life is believed to be stressful (Molet et al., 2014). However, the duration of separation did not exceed 15 minutes per day, and C rats were also manipulated by the experimenter and separated from the mother. The BW recovered at PND60.

Chronic immobilization of hind limbs from birth to PND28 altered muscle development. A severe muscle atrophy was observed at PND28, which persisted at PND60 in spite of a one month-period of free movements recovery. When immobilization is endured during adulthood, a decrease in MWW is also observed, but relative value (soleus mass to body mass ratio) returned to normal within a few days (Lawler et al., 2012; Widrick et al., 2008). Thus, it seems that during development, a critical period exists, where muscle activity is required to allow typical muscle development.

It is classically assumed that atrophy can be explained by a lower CSA. The CSA of SMR rats was decreased at PND28 with respect to C rats. The reduced CSA is classically reported after disuse, in adults as in young rodents. For instance, hind limb unloading from PND8 to PND17 resulted in a decrease in CSA (Huckstorf et al., 2000), but the persistence of this effect after reloading has not been explored. Kawano et al. (Kawano et al., 2008) showed that hind limb unloading from PND4 to PND90, i.e. until adulthood, induced a 69% decrease in soleus fiber CSA, that was not totally reversed after a 3-month period of recovery. In the present work, at PND60, the decrease in CSA was abolished, and large fibers were even more frequently encountered. Thus, CSA recovered with a one month-period of normal sensorimotor activity. Serradj et al. (Serradj et al., 2013) has also provided evidence for a recovery in mice submitted to unloading from birth to P21. On the other hand, the CSA for triceps surae myofibers was still reduced at P90 in SMR rats compared with controls (Coq et al., 2008; Delcour et al., 2018a; Marcuzzo et al., 2008) whereas quadriceps and hamstrings CSA were unchanged. This discrepancy suggests that recovery to SMR might be dependent on the muscle phenotype, slow postural muscles such as soleus muscle being more likely to return to a normal phenotype when postural function is resumed.

In the present study, the two parameters, i.e. MWW and CSA, seem to be disconnected since the decrease in MWW is far higher than the decrease in CSA, in particular at PND60 (~-40% vs -14% respectively), and CSA recovered but not MWW. The discrepancy between atrophy and CSA could be the

result of a decrease in the number of myofibers. This hypothesis is sustained by many studies showing that short-term immobilization of muscles leads to apoptosis (for instance: (Hao et al., 2011; Slimani et al., 2012; Suh et al., 2019). This effect is most noticeable at PND60, likely due to a fiber muscle injury induced by the unusual increase in mechanical stress after immobilization (Andrianjafiniony et al., 2010; Flück et al., 2003). An increase in Pax7 immunostaining has been observed in the soleus agonist (gastrocnemius muscle) of adult rats submitted to SMR during development, confirming the existence of lesional tissue (Delcour et al., 2018a).

The discrepancy between atrophy and CSA could also be explained by a decrease in the non-muscle fiber component, namely the connective tissue. However, this hypothesis is in contradiction with studies showing that a thickening of perimysium is observed in adult rats submitted to immobilization (Delcour et al., 2018a; Järvinen et al., 2002; Slimani et al., 2012) as well as in CP patients (de Bruin et al., 2014). We previously showed that SMR leads to increased connective tissue within the triceps surae, quadriceps and hamstrings. Collagen type I showed a small increase, but connective tissue growth factor (CTGF) increased significantly after SMR (Coq et al., 2008; Marcuzzo et al., 2008).

We have shown that SMR profoundly affected tetanic tension (P_0) at PND28 as well as at PND60 (in particular in female rats). Proprioceptive information from muscle afferent fibers appears crucial in the regulation of contraction force. For instance, during hind limb unloading in adult rats, a situation that strongly reduces afferent input from hind limbs, maximal tetanic tension is strongly reduced, and activation of IA afferent fibers by tendon vibration significantly attenuates this decrease (Falempin and Fodili-In-Albon, 1999). The decline in P_0 may reflect the muscle atrophy, a selective loss of contractile proteins (and thus a decrease in the cross-bridge number) and/or a decrease in the force generated per cross-bridge (McDonald and Fitts, 1995). The specific tension (i.e. P_0 to MWW ratio) was unchanged at PND28 and PND60, suggesting that force loss is proportional to muscle atrophy, whereas no change was reported in actin content. At a more integrated level also, the force developed on the grip test was decreased but remained unchanged when normalized to body weight.

2. Kinetic parameters are not affected by SMR

Muscle phenotype is characterized by a delay in muscle maturation with persistence of small amount of neonatal isoform of MHC proteins at PND28 and a lower proportion of MHC I, but the difference was weak and did not persist at PND60. It should be noted that in some SMR rats, small amounts of MHC IIB were detected while this isoform is typically absent in the control soleus muscle. Other authors have already shown that a various form of disuse in the postnatal period results in altered muscle phenotype, towards a decrease in type I MHC and retention of small amounts of neonatal isoform (Adams et al., 1999; Kawano et al., 2010). Picquet and collaborators (Picquet et al., 1998) has shown that immobilization of hind limbs from P6 to P12, i.e. before the appearance of monosynaptic innervation delays the postnatal maturation (persistence of neonatal isoforms); whereas, when immobilization occurs between PND17 to PND23, i.e. under monosynaptic innervation, the muscle evolves toward a faster phenotype. Thus, the maturation of muscle phenotype is dependent on neural factors. The moderate changes in kinetic parameters and muscle phenotype are striking in view of the persistent changes in contractile properties.

In adult rats, it has been shown that afferent input is a major determinant of muscle mass whereas phenotype is linked to motor command. Indeed, in rats submitted to hind limb unloading, activation of proprioceptive fibers by pressure applied on the plantar sole or by tendinous vibration can prevent at least partially muscle atrophy (De-Doncker et al., 2000; Falempin and Fodili-In-Albon, 1999). On the other hand, changes in the motor drive, either suppression by tetrodotoxin (Michel et al., 1996) or electrostimulation with a tonic pattern (Dupont et al., 2011; Leterme and Falempin, 1994; Pette and Vrbová, 2017) prevent phenotypic changes due to unloading but do not affect muscle mass. Taken together, it seems that in our model of SMR, the paucity of movements (and thus of proprioceptive feedback), both qualitatively and quantitatively, is the key factor for the maturation of muscle properties, the role of the decrease in motor drive being less prominent.

3) The sensorimotor performance is altered in SMR rats

The first postnatal weeks are important for integration of sensory input and maturation of spinal reflexes (Brumley et al., 2015). Walton and collaborators (Walton et al., 1992) have reported that the period extending from postnatal days 8–13 is a critical period for motor performance, in which animals are the most sensitive to hind limb unloading. Moreover, when pups were unloaded from PND 13–31, abnormal walking patterns persisted into adulthood. The first postnatal weeks correspond to a period of maturation and refinement of the spinal circuits, and of myofiber monoinnervation setting up. The performance on the rotarod, a test that requires a good coordination, showed a dramatic alteration without any sign of recovery one month after the end of hind limb immobilization. Locomotor parameters were also disturbed after SMR. Changes were less pronounced but maximum contact values were still significantly different from controls at P56. These enduring deficits, that contrast with the fact that motor activity is quantitatively normal or even increased from PND28 to PND56, are the sign of a functional disorganization of sensorimotor networks. They suggest that proprioceptive feedback is essential not only to control atrophy, but also for development of a coordinated locomotor pattern during the early postnatal development (Brumley et al., 2015). We also examined the withdrawal reflex and showed that its threshold was lowered, but whether this result may be due to reduced and altered somatosensory feedback, spinal hyperexcitability or in to supraspinal regulation of postural control is difficult to established. Our results suggest that the growth delay, and thus the lower body weight, can participate to the decrease in threshold.

Sensorimotor activity plays a crucial role in formation and refinement of synapses and neural networks. The discrepancy between the rather moderate degradation in muscle properties and the striking impairments in motor outputs, particularly on the rotarod, suggests that a disorganization of neuronal circuits at the spinal and/or supraspinal level is involved in behavioral changes. Indeed, we previously showed that SMR has a strong impact on supraspinal structures, particularly the cerebral cortex where it degraded the topographical organization of the somatosensory hind limb maps, reduced cortical areas devoted to both somatosensory and motor hind limb representations and altered response properties, such as enlarged tactile receptive fields and reduced electrical thresholds to produce movements, and cortical hyperexcitability as well (Delcour et al., 2018a; Delcour et al., 2018b). At the spinal level, the electrophysiological approach has shown that the depression of H reflex, that is classically observed in C rats when stimulation rate increases, disappeared. This hyperreflexia is a sign of spasticity and is indicative

of hyperexcitability within the spinal cord. Such a phenomenon had already been demonstrated in the same model of SMR on the flexor digitorum brevis muscle (Delcour et al., 2018a). In human, spasticity is usually caused by lesions of the CNS, such as spinal cord injury or stroke. In children, it is a common feature of CP (Jeffries et al., 2016). In the present study, spasticity can occur without brain damage. Our results once more emphasize the role of sensorimotor experience in maturation of spinal circuitry.

CONCLUSION

Our results showed that SMR from birth to PND28 delayed muscle maturation and altered soleus muscle properties. SMR led also to hyperexcitability of the spinal cord. Our data support the idea that proprioceptive feedback or reafference is at least as important as the quantity of motor activity in promoting typical development of motor function. It is also difficult to determine whether muscle atrophy is the cause or the result of altered sensorimotor experience . The impaired control and coordination of motor activity in the absence of neurological disorder is a characteristic of developmental coordination disorders (DCD) (Vaivre-Douret, 2014). A better knowledge of the interplay between hypoactivity, muscle properties and central motor commands may provide therapeutic perspectives for children with DCD or other related neurodevelopmental disorders.

Funding: This study was funded by Ministère de l'Enseignement Supérieur et de la Recherche, la Fondation Motrice, Lille University.

Declarations of interest: none

Authors' contributions: **Marie-Hélène Canu**: Conceptualization, Formal analysis, Investigation, Writing - Original Draft, Visualization, Supervision. **Valérie Montel**: Investigation. **Julie Dereumetz**: Investigation. **Tanguy Marqueste**: Investigation. **Patrick Decherchi**: Investigation. **Jacques-Olivier Coq**: Conceptualization, Investigation, Writing - Review & Editing. **Erwan Dupont**: Methodology, Investigation. **Bruno Bastide**: Methodology, Writing - Review & Editing.

Acknowledgements: Experiments were performed in the Eurasport facility of Lille University and ISM Marseille.

Reference list

Adams, G.R., McCue, S.A., Zeng, M., Baldwin, K.M., 1999. Time course of myosin heavy chain transitions in neonatal rats: importance of innervation and thyroid state. The American journal of physiology 276, R954-961.

Andrianjafiniony, T., Dupré-Aucouturier, S., Letexier, D., Couchoux, H., Desplanches, D., 2010. Oxidative stress, apoptosis, and proteolysis in skeletal muscle repair after unloading. Am J Physiol Cell Physiol 299, C307-315.

Biotteau, M., Albaret, J.M., Chaix, Y., 2020. Developmental coordination disorder. Handbook of clinical neurology 174, 3-20.

Blivis, D., Haspel, G., Mannes, P.Z., O'Donovan, M.J., Iadarola, M.J., 2017. Identification of a novel spinal nociceptive-motor gate control for Aδ pain stimuli in rats. Elife 6.

Brumley, M.R., Kauer, S.D., Swann, H.E., 2015. Developmental plasticity of coordinated action patterns in the perinatal rat. Dev Psychobiol 57, 409-420.

Canu, M.H., Fourneau, J., Coq, J.O., Dannhoffer, L., Cieniewski-Bernard, C., Stevens, L., Bastide, B., Dupont, E., 2019. Interplay between hypoactivity, muscle properties and motor command: How to escape the vicious deconditioning circle? Annals of physical and rehabilitation medicine 62, 122-127.

Coq, J.O., Barr, A.E., Strata, F., Russier, M., Kietrys, D.M., Merzenich, M.M., Byl, N.N., Barbe, M.F., 2009. Peripheral and central changes combine to induce motor behavioral deficits in a moderate repetition task. Exp Neurol 220, 234-245.

Coq, J.O., Kochmann, M., Lacerda, D.C., Khalki, H., Delcour, M., Toscano, A.E., Cayetanot, F., Canu, M.H., Barbe, M.F., Tsuji, M., 2019. From cerebral palsy to developmental coordination disorder: Development of preclinical rat models corresponding to recent epidemiological changes. Annals of physical and rehabilitation medicine.

Coq, J.O., Strata, F., Russier, M., Safadi, F.F., Merzenich, M.M., Byl, N.N., Barbe, M.F., 2008. Impact of neonatal asphyxia and hind limb immobilization on musculoskeletal tissues and S1 map organization: implications for cerebral palsy. Exp Neurol 210, 95-108.

Cousins, M., Smyth, M.M., 2003. Developmental coordination impairments in adulthood. Hum Mov Sci 22, 433-459.

De-Doncker, L., Picquet, F., Falempin, M., 2000. Effects of cutaneous receptor stimulation on muscular atrophy developed in hindlimb unloading condition. J Appl Physiol (1985) 89, 2344-2351.

de Bruin, M., Smeulders, M.J., Kreulen, M., Huijing, P.A., Jaspers, R.T., 2014. Intramuscular connective tissue differences in spastic and control muscle: a mechanical and histological study. PLoS One 9, e101038.

Delcour, M., Massicotte, V.S., Russier, M., Bras, H., Peyronnet, J., Canu, M.H., Cayetanot, F., Barbe, M.F., Coq, J.O., 2018a. Early movement restriction leads to enduring disorders in muscle and locomotion. Brain pathology (Zurich, Switzerland) 28, 889-901.

Delcour, M., Russier, M., Castets, F., Turle-Lorenzo, N., Canu, M.H., Cayetanot, F., Barbe, M.F., Coq, J.O., 2018b. Early movement restriction leads to maladaptive plasticity in the sensorimotor cortex and to movement disorders. Sci Rep 8, 16328.

Drzymala-Celichowska, H., Karolczak, J., Redowicz, M.J., Bukowska, D., 2012. The content of myosin heavy chains in hindlimb muscles of female and male rats. Journal of physiology and pharmacology : an official journal of the Polish Physiological Society 63, 187-193.

Drzymała-Celichowska, H., Krutki, P., 2015. Slow motor units in female rat soleus are slower and weaker than their male counterparts. Journal of muscle research and cell motility 36, 287-295.

Dupont, E., Cieniewski-Bernard, C., Bastide, B., Stevens, L., 2011. Electrostimulation during hindlimb unloading modulates PI3K-AKT downstream targets without preventing soleus atrophy and restores slow phenotype through ERK. Am J Physiol Regul Integr Comp Physiol 300, R408-417.

Falempin, M., Fodili-In-Albon, S., 1999. Influence of brief daily tendon vibration on rat soleus muscle in non-weight-bearing situation. J Appl Physiol (1985) 87, 3-9.

Flück, M., Chiquet, M., Schmutz, S., Mayet-Sornay, M.H., Desplanches, D., 2003. Reloading of atrophied rat soleus muscle induces tenascin-C expression around damaged muscle fibers. Am J Physiol Regul Integr Comp Physiol 284, R792-801.

Hao, Y., Jackson, J.R., Wang, Y., Edens, N., Pereira, S.L., Alway, S.E., 2011. beta-Hydroxy-beta-methylbutyrate reduces myonuclear apoptosis during recovery from hind limb suspension-induced muscle fiber atrophy in aged rats. Am J Physiol Regul Integr Comp Physiol 301, R701-715.

Hermans, G., Van den Berghe, G., 2015. Clinical review: intensive care unit acquired weakness. Crit Care 19, 274.

Huckstorf, B.L., Slocum, G.R., Bain, J.L., Reiser, P.M., Sedlak, F.R., Wong-Riley, M.T., Riley, D.A., 2000. Effects of hindlimb unloading on neuromuscular development of neonatal rats. Brain Res Dev Brain Res 119, 169-178.

Järvinen, T.A., Józsa, L., Kannus, P., Järvinen, T.L., Järvinen, M., 2002. Organization and distribution of intramuscular connective tissue in normal and immobilized skeletal muscles. An immunohistochemical, polarization and scanning electron microscopic study. Journal of muscle research and cell motility 23, 245-254.

Jeffries, L., Fiss, A., McCoy, S.W., Bartlett, D.J., 2016. Description of Primary and Secondary Impairments in Young Children With Cerebral Palsy. Pediatr Phys Ther 28, 7-14.

Kawano, F., Goto, K., Wang, X.D., Terada, M., Ohira, T., Nakai, N., Yoshioka, T., Ohira, Y., 2010. Role(s) of gravitational loading during developing period on the growth of rat soleus muscle fibers. J Appl Physiol (1985) 108, 676-685.

Kawano, F., Takeno, Y., Nakai, N., Higo, Y., Terada, M., Ohira, T., Nonaka, I., Ohira, Y., 2008. Essential role of satellite cells in the growth of rat soleus muscle fibers. Am J Physiol Cell Physiol 295, C458-467.

Koukourikos, K., Tsaloglidou, A., Kourkouta, L., 2014. Muscle atrophy in intensive care unit patients. Acta Inform Med 22, 406-410.

Lawler, J.M., Kwak, H.B., Kim, J.H., Lee, Y., Hord, J.M., Martinez, D.A., 2012. Biphasic stress response in the soleus during reloading after hind limb unloading. Med Sci Sports Exerc 44, 600-609.

Leterme, D., Falempin, M., 1994. Compensatory effects of chronic electrostimulation on unweighted rat soleus muscle. Pflugers Arch 426, 155-160.

Li, Y.C., Wu, S.K., Cairney, J., Hsieh, C.Y., 2011. Motor coordination and health-related physical fitness of children with developmental coordination disorder: a three-year follow-up study. Research in developmental disabilities 32, 2993-3002.

Luhmann, H.J., Sinning, A., Yang, J.W., Reyes-Puerta, V., Stüttgen, M.C., Kirischuk, S., Kilb, W., 2016. Spontaneous Neuronal Activity in Developing Neocortical Networks: From Single Cells to Large-Scale Interactions. Front Neural Circuits 10, 40.

Marcuzzo, S., Dutra, M.F., Stigger, F., do Nascimento, P.S., Ilha, J., Kalil-Gaspar, P.I., Achaval, M., 2008. Beneficial effects of treadmill training in a cerebral palsy-like rodent model: walking pattern and soleus quantitative histology. Brain Res 1222, 129-140.

Martinov, T., Mack, M., Sykes, A., Chatterjea, D., 2013. Measuring changes in tactile sensitivity in the hind paw of mice using an electronic von Frey apparatus. Journal of visualized experiments : JoVE, e51212.

Mayeuf-Louchart, A., Hardy, D., Thorel, Q., Roux, P., Gueniot, L., Briand, D., Mazeraud, A., Bougle, A., Shorte, S.L., Staels, B., Chretien, F., Duez, H., Danckaert, A., 2018. MuscleJ: a high-content analysis method to study skeletal muscle with a new Fiji tool. Skelet Muscle 8, 25.

McDonald, K.S., Fitts, R.H., 1995. Effect of hindlimb unloading on rat soleus fiber force, stiffness, and calcium sensitivity. J Appl Physiol (1985) 79, 1796-1802.

Michel, R.N., Parry, D.J., Dunn, S.E., 1996. Regulation of myosin heavy chain expression in adult rat hindlimb muscles during short-term paralysis: comparison of denervation and tetrodotoxin-induced neural inactivation. FEBS Lett 391, 39-44.

Miranda, D.L., Putman, M., Kandah, R., Cubria, M., Suarez, S., Nazarian, A., Snyder, B., 2016. A pediatric animal model to evaluate the effects of disuse on musculoskeletal growth and development. J Biomech 49, 3549-3554.

Molet, J., Maras, P.M., Avishai-Eliner, S., Baram, T.Z., 2014. Naturalistic rodent models of chronic early-life stress. Dev Psychobiol 56, 1675-1688.

Pette, D., Vrbová, G., 2017. The Contribution of Neuromuscular Stimulation in Elucidating Muscle Plasticity Revisited. Eur J Transl Myol 27, 33-39.

Picquet, F., Falempin, M., 2003. Compared effects of hindlimb unloading versus terrestrial deafferentation on muscular properties of the rat soleus. Exp Neurol 182, 186-194.

Picquet, F., Stevens, L., Butler-Browne, G.S., Mounier, Y., 1998. Differential effects of a six-day immobilization on newborn rat soleus muscles at two developmental stages. Journal of muscle research and cell motility 19, 743-755.

Rosenbaum, P., Paneth, N., Leviton, A., Goldstein, M., Bax, M., Damiano, D., Dan, B., Jacobsson, B., 2007. A report: the definition and classification of cerebral palsy April 2006. Developmental medicine and child neurology. Supplement 109, 8-14.

Serradj, N., Picquet, F., Jamon, M., 2013. Early postnatal motor experience shapes the motor properties of C57BL/6J adult mice. Eur J Neurosci 38, 3281-3291.

Slimani, L., Micol, D., Amat, J., Delcros, G., Meunier, B., Taillandier, D., Polge, C., Béchet, D., Dardevet, D., Picard, B., Attaix, D., Listrat, A., Combaret, L., 2012. The worsening of tibialis anterior muscle atrophy during recovery post-immobilization correlates with enhanced connective tissue area, proteolysis, and apoptosis. American journal of physiology. Endocrinology and metabolism 303, E1335-1347.

Suh, H.R., Park, E.H., Moon, S.W., Kim, J.W., Cho, H.Y., Han, H.C., 2019. Apoptotic changes in a full-lengthened immobilization model of rat soleus muscle. Muscle Nerve 59, 263-269.

Toursel, T., Bastide, B., Stevens, L., Rieger, F., Mounier, Y., 2000. Alterations in contractile properties and expression of myofibrillar proteins in wobbler mouse muscles. Exp Neurol 162, 311-320.

Vaivre-Douret, L., 2014. Developmental coordination disorders: state of art. Neurophysiol Clin 44, 13-23.

Vaivre-Douret, L., Lalanne, C., Golse, B., 2016. Developmental Coordination Disorder, An Umbrella Term for Motor Impairments in Children: Nature and Co-Morbid Disorders. Frontiers in Psychology 7.

Walton, K.D., Lieberman, D., Llinas, A., Begin, M., Llinas, R.R., 1992. Identification of a critical period for motor development in neonatal rats. Neuroscience 51, 763-767.

Westerga, J., Gramsbergen, A., 1993. Development of locomotion in the rat: the significance of early movements. Early human development 34, 89-100.

Widrick, J.J., Maddalozzo, G.F., Hu, H., Herron, J.C., Iwaniec, U.T., Turner, R.T., 2008. Detrimental effects of reloading recovery on force, shortening velocity, and power of soleus muscles from hindlimb-unloaded rats. Am J Physiol Regul Integr Comp Physiol 295, R1585-1592.